RNA Sequencing to Explore Dominant Isoform Switch During CCR6+ Memory T Cell Activation

Shanrong Zhao (Shanrong_zhao@yahoo.com)
Pfizer (United States)
Alexander Barron
Pfizer (United States)
Ken Dower
Pfizer (United States)

Research Article

Keywords: Alternative splicing, RNA-seq, isoform switch, T cell activation

Posted Date: January 12th, 2021

DOI: https://doi.org/10.21203/rs.3.rs-140817/v1

Abstract

Alternative splicing (AS) is an essential, but under-investigated component of T-cell function during immune responses. Recent developments in RNA sequencing (RNA-seq) technologies, combined with the advent of computational tools, have enabled transcriptome-wide studies of AS at an unprecedented scale and resolution. In this paper, we analysed AS in an RNA-seq dataset previously generated to investigate the expression changes during T-cell maturation and antigen stimulation. Eight genes were identified with their most dominant isoforms switched during T cell activation. Of those, seven genes either directly control cell cycle progression or are oncogenes. We selected CDKN2C, FBXO5, NT5E and NET1 for discussion of the functional importance of AS of these genes. Our case study demonstrates that combining AS and gene expression analyses derives greater biological information and deeper insights from RNA-seq datasets than gene expression analysis alone.

Introduction

Alternative splicing (AS) rapidly converts the product of a single gene from one isoform to another[1]. Thus, AS is crucial for generating immediate biological responses, and allows one gene to encode instructions for making multiple proteins with distinct functions[2]. CD45 is a good example. Its transcript undergoes AS (Supplementary **Fig. S1**) to generate proteins with disparate functions[3]. For example, T and B cells express separate isoforms which change as the cells undergo activation and differentiation[4]. The large CD45 isoforms expressed by naïve T cells are a stronger break on activation than the shorter CD45 isoform, CD45RO, which is expressed by memory T cells. AS influences the risk of several diseases, including neurodegenerative disorders, cancer, immune and infectious diseases, cardiovascular and metabolic diseases[2,5–7]. Studying AS holds promise for the development of clinical biomarkers and novel therapies in this era of precision medicine[8].

AS isoforms were historically characterized by reverse transcription polymerase chain reaction (RT-PCR) and expressed sequence tags (ESTs). Experimental approaches graduated to the genome-wide scale with the development of AS microarrays. These successfully identified AS across tissues, cellular states, and species[9,10]. However, these technologies have low throughput (RT-PCR and ESTs), high noise (ESTs and AS microarrays), or only capture known splicing events (RT-PCR and splicing microarray). More recently, RNA sequencing (RNA-seq) has improved the study of AS in several ways[11]. Compared with microarray-based transcriptome profiling, RNA-seq has a wider dynamic range and avoids some of the technical limitations such as varying probe performance and cross-hybridization[12], and provides novel insights into AS[13]. Computational tools such as MISO[14], MAJIQ[15], rMATs[16] and LeafCut[17] have been developed to detect both known and novel splicing events from RNA-seq data. Other tools such as RSEM[18], Kallisto[19], and Salmon[20] can be applied to analyze and quantify known or annotated transcript isoforms.

Vitting-Seerup et al characterized isoform switching from > 5,500 cancer patients' RNA-seq data covering 12 solid cancer types and identified many isoform switches as powerful biomarkers: 31 switches were

highly predictive of patient survival independent of cancer types[21]. Their study indicates that isoform switches with predicted functional consequences are common and important in dysfunctional cells, which in turn means that expression change should be analyzed at the isoform level. Our previous study also demonstrated additional mechanistic insights can be gained through interrogation of AS in addition to conventional gene-level analysis of RNA-seq data[22]. Most recently, Kahraman et al have analyzed isoform-specific protein–protein interaction disruptions in 1,209 cancer samples covering 27 different cancer types from the Pan-Cancer Analysis of Whole Genomes (PCAWG) project, and identified a number of cancer-specific Most Dominant Transcripts (cMDT) [23].

Our understanding of immune response regulation by AS is scant compared to oncology[24]. AS microarray profiling identified extensive novel AS changes in activated T cells suggesting a key role for AS in regulating the mammalian immune response[25]. The types of genes controlled by AS during T-cell activation are different from those governed by changes in transcript levels; AS is associated with cell-cycle regulation, whereas alterations in transcript abundance dictate changes in immune defense and cytoskeletal architecture[25]. Previously, we compared the transcriptomes of activated CCR6 + memory T-cells by RNA-seq and microarray. A plethora of differentially expressed genes were identified by both platforms, but RNA-seq was superior in differentiating biologically critical isoforms[12]. Prior research defined transcriptional changes that regulate protein expression during T-cell maturation and antigen stimulation. Here, we build upon this work by using the same RNA-seq dataset to globally analyze AS during T-cell stimulation.

Materials And Methods

RNA-seq dataset.

The raw RNA-seq data from this study was downloaded from the NCBI sequence read archive under the accession number SRP026389, and described in detail elsewhere[12]. Briefly, human PBMCs was purified from a healthy donor, and then CD4+ memory T cells were purified from PBMCs through negative selection using the memory CD4+ T cell isolation kit (Miltenyi) followed by positive selection with anti-CCR6/biotin conjugates and anti-biotin magnetic beads (Miltenyi). Purified CCR6+ T cells were stimulated with anti-CD3 and anti-CD28 coated beads (Miltenyi). RNA was prepared from resting and stimulated T cells at different time points over a time course of 3 days. There was a total of six time points, with two biological replicates per time point (**Fig. 1A**).

Isoform quantification and switch.

RNA-seq based transcriptome profiling was performed by the Illumina HiSeq™ 2000 platform. Raw sequencing reads were mapped by Salmon[20] 0.12.0 to the human genome GRCh38 and Gencode Release 29, and then a counting of matrix of 200,000 (transcripts) x 12 (samples) was generated as inputs for detecting isoform switch. All transcripts that did not express across RNA samples were filtered out first. Then those protein-coding genes with two to five expressed isoforms were kept for further analysis. The

protocol for isoform switch is depicted in **Fig. 1B** and **1C**. First, the relative abundance (**Fig 1C**) of different isoforms was calculated from their corresponding expression levels (**Fig 1B**) at each time point. Then the most dominant isoform was identified at each time point if there exists a one. All isoforms are sorted in a descending order by their relative abundance, and the top isoform is the dominant one if the relative abundance difference between the top two isoforms is greater than 0.3. Otherwise the top one is not a dominant isoform. In **Fig. 1C**, all dominant isoforms are colored in red circle, and the size of circles represents relative abundance of individual isoform at each time point. It is noted that at 6 and 24 hours, there are no dominant isoforms because the expression levels for the top two isoforms are too close. The reason for us to check the difference between the top two isoforms is to ensure the top one is indeed dominant. Isoform switch occurs if the dominant isoforms differ across time points. The list of candidate genes with potential isoform switch will be further checked using the Omicsoft genome browser, and only those isoform switches with strong evidence (i.e. raw sequence read coverage) are reported.

Protein sequence analysis and comparison.

Predicted protein sequences of each isoform were run through the InterPro (https://www.ebi.ac.uk/interpro/) and Clustal Omega (https://www.ebi.ac.uk/Tools/msa/clustalo/) tools available from the EMBL-EBI using default settings[26,27].

Results

QC of RNA-seq data.

On average, 50 million paired-end reads were sequenced per sample, and related QC metrices are shown in Supplementary **Fig. S2**. There is a total of 12 samples across all six time points, with two replicates per time point. It was a high-quality dataset in terms of read mapping and counting summaries (**Fig. S2A** and **Fig. S2B**). All samples clearly clustered by time points (**Fig. S2C** and **Fig. S2D**), as was expected and consistent with previous differential analysis[12].

Isoform switch during T cell activation.

The isoform quantification was performed by using the computational algorithm Salmon[20]. By applying the isoform switch protocol described in the Methods Section, we identified eight genes with the most dominant isoform switching during T cell activation (Table 1 and Supplementary **Fig. S3**). We wanted to determine the functional relevance of the isoform switches in Table 1. Consistent with previously published data linking AS to cell cycle regulation[25], seven of these eight genes either directly control cell cycle progression or are oncogenes. CDKN2C inhibits the activity of the cyclin D-CDK6 complex thus blocking the G1-to-S phase transition[28]. CENPM is a necessary component of the centromere, and conditional deletion halts cell division leading to cell death[29,30]. FBXO5 controls multiple cell cycle transitions as well as homologous DNA repair[31–33]. Methylation of piRNAs by HENMT1 is required for transposable element repression during germ cell division[34]. NET1 directly sequesters the phosphatase

Cdc14 to allow cyclin-dependent kinase activity throughout the cell cycle[35–37]. SHLD1 is a component of the shieldin complex responsible for non-homologous end joining in the TP53 DNA damage repair response[38,39]. UNG is the major nuclear glycosylase responsible for removing mutagenic uracil from DNA during base excision repair and is necessary for class-switch recombination in B cells[40,41]. We selected CDKN2C, FBXO5, NT5E and NET1 for further exploration.

Table 1
Eight genes with isoform switch during T cell activation

Gene	Description	Location	Type
CDKN2C	cyclin dependent kinase inhibitor 2C	Nucleus	transcription regulator
CENPM	centromere protein M	Cytoplasm	other
FBXO5	F-box protein 5	Nucleus	enzyme
HENMT1	HEN methyltransferase 1	Cytoplasm	enzyme
NET1	neuroepithelial cell transforming 1	Nucleus	other
NT5E (CD73)	5'-nucleotidase ecto	Plasma Membrane	phosphatase
SHLD1	shieldin complex subunit 1	Nucleus	other
UNG	uracil DNA glycosylase	Nucleus	enzyme

Isoform switch in CDKN2C (Cyclin-Dependent Kinase Inhibitor 2C)/p18(INK4C).

CDKN2C inhibits T cell proliferation in response to TCR stimulation by binding to CDK6. This block is overcome through CD28 costimulation[42,43]. In resting T cells, the isoform CDKN2C-202 is dominant. Within two hours of activation through both the CD3 and CD28 pathways, levels of this isoform rapidly diminish. Then at 72 hours post-activation expression of the CDKN2C-203 isoform increases to predominate (Fig. 2A). Based on these data we hypothesized that the CDKN2C-202 isoform lacked the domains necessary to inhibit CDK6 thus leaving non-terminal effector T cells primed for proliferation in response to TCR stimulation.

CDKN2C encodes five ankyrin repeats[44]. The second and third form the inhibitory interface with CDK6[45]. Alignment of the splice variants demonstrated that the CDKN2C-203 isoform has a single amino acid truncation of the fourth ankyrin domain and completely lacks the fifth ankyrin domain (Fig. 2B). Thus, both CDKN2C isoforms possess the second and third ankyrin domains, which are necessary for CDK6 binding. Another hypothesis we explored was that the CDKN2C-203 variant encodes an unstable CDKN2C isoform. Truncation mutants of CDKN2C lacking the fifth ankyrin domain appear unstable as this deletion construct produces little protein[44,46]. This CDKN2C isoform switch is likely important to CDK6 regulation and the generation of adaptive immunity while preventing lymphomas and inflammatory diseases[42,43].

Isoform switch in FBXO5/FBX5 (F-box protein 5)/EMI1 (Early Mitotic Inhibitor 1).

FBXO5 is encoded at the minus strand, and has two expressed protein coding isoforms, i.e. FBXO5-201 and FBXO5-202 (Fig. 3A). FBXO5-202 is the dominant isoform at early time points, but FBXO5-201 becomes the dominant isoform at 72hr (Fig. 3A). The high expression level of FBXO5-201 at 72hr is evident from the sequence read coverage profile (Fig. 3B). Note FBXO5 also has a non-coding isoform FBXO5-203 that is barely expressed. After protein translation, FBXO5-201 is 46 amino acids longer than FBXO5-202 in the N-terminus. These 46 amino acids encode three key features: a putative signal peptide (Fig. 3C) and two potential Cdk phosphorylation sites. As a member of the F-box protein family, FBXO5 has several protein-protein interactions that could be affected by this isoform switch[31–33]. Despite a large body of work on FBXO5, the functional consequences of these three features are unknown.

FBXO5 is involved in the osteogenic differentiation of mesenchymal stem cells (MSCs)[47]. The expression of FBXO5 was upregulated after osteogenic induction in human periodontal ligament stem cells (hPDLSCs). FBXO5 knockdown attenuated migration, inhibited alkaline phosphatase (ALP) activity and mineralization, and decreased RUNX2, OSX, and OCN expression, while the overexpression of two transcript isoforms significantly accelerated migration, enhanced ALP activity and mineralization, and increased RUNX2, OSX, and OCN expression in hPDLSCs. It was concluded that both FBXO5-201 and FBXO5-202 promoted the migration and osteogenic differentiation potential of hPDLSCs, which identified a potential target for improving periodontal tissue regeneration. However, whether the two isoforms have different biological roles, especially during T cell activation, remains unclear.

Isoform switch in NT5E (5'-nucleotidase ecto)/CD73 (cluster of differentiation 73).

The protein encoded by this gene is a plasma membrane enzyme that catalyzes the conversion of extracellular AMP to adenosine. The encoded protein is used as a determinant of lymphocyte differentiation. Defects in this gene can lead to the calcification of joints and arteries. The two CCDS-validated transcripts of NT5E are NT5E-201 and NT5E-203, which differ with respect to the presence of exon 7 in NT5E-201 (Fig. 4). NT5E-201 encodes canonical CD73, denoted as CD73L, while the NT5E-203 transcript is predicted to encode a shorter protein CD73S. Human CD73S lacks amino acids 404–453, encoded by the missing exon 7. The dominant isoform is NT5E-203 at 2 and 4hr, but it is NT5E-201 at 0 and 72hr (Fig. 4). CD73S was expressed at low abundance in normal human tissues but was significantly up-regulated in cirrhosis and hepatocellular carcinoma (HCC)[48]. These two human isoforms exhibited functional differences, such that ectopic expression of canonical CD73L in human HepG2 cells was associated with decreased expression of the proliferation marker Ki67, whereas CD73S expression did not have an effect on Ki67 expression[48]. CD73S was glycosylated, catalytically inactive, unable to dimerize, and complexed intracellularly with the endoplasmic reticulum chaperone calnexin. Furthermore, CD73S negatively regulates CD73L activity and protein expression in a proteasome-dependent manner[48]. It remains unclear the roles of CD73L and CD73S in T cell activation, though new data suggest that CD8 + CD73 + T cells may be especially important mediators of immunosuppression in human head and neck cancer[49].

Isoform switch in NET1 (Neuroepithelial cell transforming 1).

The gene NET1 is part of the family of Rho guanine nucleotide exchange factors. Members of this family activate Rho proteins by catalyzing the exchange of GDP for GTP. The protein encoded by this gene interacts with RhoA within the cell nucleus and may play a role in repairing DNA damage after ionizing radiation. Alternative splicing results in multiple transcript variants that encode different protein isoforms. Compared with NET1-202, the expression for NET1-201 is low at early time points but increases significantly and become the dominant isoform at 24 and 72hr. NET1-201 and NET1-202 display distinct exon usage in their 5' ends (Fig. 5A). We performed Clustal Omega alignment of the predicted protein sequences of NET1-201 and – 202, and found that NET1-202 completely lacks the first nuclear localization sequences (NLS) in its N-terminus and that there is poor conservation of the second NLS (Fig. 5B). These NLSs are functionally important as oncogenic NET1 lacks the N-terminal 145 amino acids encoding the NLS, and deletion of the two NLS redistributes NET1 from the nucleus to the cytoplasm[50,51]. The dominance of the NLS-containing NET1-201 splice variant at 24- and 72-hours post-stimulation suggests that nuclear sequestration of Cdc14 by NET1 is important for TCR-driven T cell proliferation and maximally effective adaptive immune responses.

The regulation of the two isoforms of NET1 by transforming growth factor-β (TGF-β) in keratinocytes has been studied, and the results emphasize the importance of NET1-202 in the short- and long-term TGF-β-mediated regulation of epithelial-to-mesenchymal transition (EMT)[52]. It was found that short-term TGF-β treatment selectively induced NET1-202 (also termed as Net1A) but not NET1-201. Interestingly, long-term TGF-β treatment resulted in Net1A protein degradation by the proteasome. Silencing of Net1A resulted in disruption of E-cadherin- and zonula occludens-1 (ZO-1)-mediated junctions, as well as expression of the transcriptional repressor of E-cadherin, Slug and the mesenchymal markers N-cadherin, plasminogen activator inhibitor-1 (PAI-1) and fibronectin, indicating that late TGF-β-induced downregulation of Net1A is involved in EMT. In conclusion, this study provides new evidence for the differential regulation of the two isoforms of the RhoA-specific GEF NET1 by TGF-β. It points out differential regulatory effects of TGF-β on the NET1A isoform, depending on the duration of the signal[52].

Discussion

Manual check to detect reliable isoform switch.

The accuracy of isoform quantification is influenced by the complexity of gene structures and caution must be taken when interpreting quantification results for short and complex isofroms[53]. It was also discovered that both sequencing depth and the relative abundance of different isoforms affect quantification accuracy. Considering the inaccuracy and uncertainty in isoform quantification, we manually check all reported isoform switches and filter out those false positives. SFNX3 (sideroflexin 3) has seven isoforms and SFXN3-201 and SFXN3-202 are the two mainly expressed forms (Supplementary **Fig. S4B**). According to Supplementary **Fig. S4A** there is an evident isoform switch, but this switch is questionable considering the two isoforms SFXN3-201 and SFXN3-202 are nearly identical. As a matter

of fact, SFXN3-202 is only 5 bp longer than SFXN3-201 at the 5' end of UTR (Exon #1), and virtually indistinguishable. Therefore, the reported isoform switch is most likely a false positive due to unreliable isoform quantification. Another example of a false isoform switch is shown in Supplementary **Fig. S5**. RAB43-201 is the dominant isoform at early time points, while RAB43-208 becomes the dominant isoform at 24 and 72 hr. Unfortunately, the high expression level of RAB43-208 at 24 and 72 hours is not supported by the read coverage profiles in **Fig. S5B** since no sequence reads are mapped to the unique exon #3 of the isoform RAB43-208.

Isoform switching in human T cells.

There is a dearth of data on the role of AS in T-cell activation and differentiation. Martinez et al[54] used RNA-seq to identify 178 exons in 168 genes exhibiting robust changes in AS during stimulation of a human T-cell line, further demonstrating the importance of AS in T-cell responses. More recently, Szabo et al. used single-cell transcriptomics (scRNA-seq) to define the heterogeneity of human T-cells from several tissues, and determine their functional responses to stimulation[55]. Their results serve as a reference of human T-cell activation in health that, through comparison, can be used to identify disease-specific T-cell activation states. Our results support the hypothesis that some genes undergo AS during T-cell activation and differentiation. Using computational tools and public data, we hypothesized functional consequences of these AS changes to T-cell responses. Ultimately, experimental validation is required to verify our proposed roles for AS in shaping human T-cell responses.

Coordinated regulation of T cell proliferation through alternative splicing.

Proliferation is a crucial part of antigen-specific adaptive immune responses[56,57], however T cell proliferation must be tightly controlled to allow optimal protective immunity while preventing excessive inflammatory destruction and leukemia/lymphoma. Consistent with a prior publication[25], seven of the eight genes that demonstrated stimulation-driven isoform switching through alternative splicing in this study regulate proliferation. Regulation of proliferation by alternative splicing and isoform switching is consistent with at least two alternative, but non-exclusive, hypotheses. First, one isoform contributes to cell cycle regulation while the other isoform is associated with normal functions of the cell. This appears to be true for NET1, where the switch from NET1-202 to NET1-201 at 24- and 72-hours post-stimulation fits with a functional refocusing of the T cell from migrating and scanning antigen-presenting cells to proliferation. Without NLS, NET1-202 is likely split evenly between the nucleus and cytoplasm where it interacts with RhoA to control cytoskeletal reorganization[58–60]. Combined signaling through the TCR and CD28 initiates T cell proliferation which is facilitated by Cdc14 sequestration of NET1-201 in the nucleus[35–37, 50,51]. So at least some of these alternative splicing events are likely due to the need to rapidly switch between functionally distinct protein isoforms encoded by the same gene during T cell activation.

A second hypothesis is that alternative splicing allows faster protein production than *de novo* transcription. This may be the case for CDKN2C. If the CDKN2C-202 isoform is unstable it may be a

relatively weak Cdk6 inhibitor thus allowing earlier cell cycle progression or proliferation at lower TCR/costimulatory signaling thresholds. As activated T cells progress through the cell cycle, Cdk6 inhibition by CDKN2C must be removed hence the low levels of both isoforms from 2 to 24 hours-post stimulation. The isoform switch to the putatively more stable CDKN2C-201 at 72 hours post-stimulation may facilitate the transition from T cell proliferation to differentiation or be part of terminal effector T cell differentiation.

Rapid isoform switching through alternative splicing of CD73 is likely necessary for T cell activation and effective adaptive immune responses.

Adenosine generation by CD73 plays both autocrine and paracrine roles in T cell activation[61]. The A2a, an inhibitory adenosine receptor, is the predominant form expressed by T cells. Signaling through the A2a adenosine receptor inhibits T cell proliferation at least partly by limiting IL-2 production[62,63]. Dendritic cells (DC) also express A2A and A2B adenosine receptors, and signaling through the A2B receptor blocks DC maturation and co-stimulation of T cells[64]. Thus, the switch in alternative splicing of CD73 during T cell activation fits with the immediate need for proliferation and differentiation. Upon recognition of cognate antigen, T cells cease migrating and form an immunological synapse with the presenting DC[65,66]. Increased expression of a catalytically inactive CD73 that complexes with and promotes degradation of CD73L through isoform switching would provide a rapid method of clearing this inhibitor of proliferation and differentiation[48]. As T cell activation is a stepwise dialogue between DC and T cell, quickly preventing suppressive adenosine accumulation in the microenvironment around DC-T cell pairs is likely critical to costimulation by CD86, IL-2 production and effective adaptive immune responses. Support for this hypothesis comes from cancer, where adenosine is a key component of suppressing the anti-tumor immune response[66,67].

Declarations

Authors Contributions

SZ conceived and designed this study. SZ performed the RNA-seq data analysis and drafted the manuscript. AMSB and KD participated in biological interpretation of isoform switching genes and in writing the manuscript. All authors approved the final manuscript.

Competing Interests

SZ, AMSB and KD are employees of Pfizer, Inc.

References

1. Pan, Q., Shai, O., Lee, L. J., Frey, B. J. & Blencowe, B. J. Deep surveying of alternative splicing complexity in the human transcriptome by high-throughput sequencing. *Nature genetics.* **40**, 1413–1415 https://doi.org/10.1038/ng.259 (2008).

2. Kim, H. K., Pham, M. H. C., Ko, K. S., Rhee, B. D. & Han, J. Alternative splicing isoforms in health and disease. *Pflugers Arch.* **470**, 995–1016 https://doi.org/10.1007/s00424-018-2136-x (2018).
3. Zikherman, J. & Weiss, A. Alternative splicing of CD45: the tip of the iceberg. *Immunity.* **29**, 839–841 https://doi.org/10.1016/j.immuni.2008.12.005 (2008).
4. Oberdoerffer, S. *et al.* Regulation of CD45 alternative splicing by heterogeneous ribonucleoprotein, hnRNPLL. *Science (New York, N.Y.).* **321**, 686–691 https://doi.org/10.1126/science.1157610 (2008).
5. Tazi, J., Bakkour, N. & Stamm, S. Alternative splicing and disease. *Biochimica et biophysica acta.* **1792**, 14–26 https://doi.org/10.1016/j.bbadis.2008.09.017 (2009).
6. Scotti, M. M. & Swanson, M. S. RNA mis-splicing in disease. *Nat Rev Genet.* **17**, 19–32 https://doi.org/10.1038/nrg.2015.3 (2016).
7. Wang, G. S. & Cooper, T. A. Splicing in disease: disruption of the splicing code and the decoding machinery. *Nat Rev Genet.* **8**, 749–761 https://doi.org/10.1038/nrg2164 (2007).
8. Zhao, S. Alternative splicing, RNA-seq and drug discovery. *Drug Discov Today.* **24**, 1258–1267 https://doi.org/10.1016/j.drudis.2019.03.030 (2019).
9. Lee, C. & Roy, M. Analysis of alternative splicing with microarrays: successes and challenges. *Genome biology.* **5**, 231 https://doi.org/10.1186/gb-2004-5-7-231 (2004).
10. Castle, J. C. *et al.* Expression of 24,426 human alternative splicing events and predicted cis regulation in 48 tissues and cell lines. *Nature genetics.* **40**, 1416–1425 https://doi.org/10.1038/ng.264 (2008).
11. Wang, Z., Gerstein, M. & Snyder, M. RNA-Seq: a revolutionary tool for transcriptomics. *Nat Rev Genet.* **10**, 57–63 https://doi.org/10.1038/nrg2484 (2009).
12. Zhao, S., Fung-Leung, W. P., Bittner, A., Ngo, K. & Liu, X. Comparison of RNA-Seq and microarray in transcriptome profiling of activated T cells. *PLoS One.* **9**, https://doi.org/10.1371/journal.pone.0078644 (2014).
13. Park, E., Pan, Z., Zhang, Z., Lin, L. & Xing, Y. The expanding landscape of alternative splicing variation in human populations. *Am J Hum Genet.* **102**, 11–26 (2018).
14. Katz, Y., Wang, E. T., Airoldi, E. M. & Burge, C. B. Analysis and design of RNA sequencing experiments for identifying isoform regulation. *Nature methods.* **7**, 1009–1015 https://doi.org/10.1038/nmeth.1528 (2010).
15. Vaquero-Garcia, J. *et al.* A new view of transcriptome complexity and regulation through the lens of local splicing variations. *eLife.* **5**, e11752 https://doi.org/10.7554/eLife.11752 (2016).
16. Shen, S. *et al.* rMATS: robust and flexible detection of differential alternative splicing from replicate RNA-Seq data. *Proceedings of the National Academy of Sciences of the United States of America.* **111**, E5593–5601 https://doi.org/10.1073/pnas.1419161111 (2014).
17. Li, Y. I. *et al.* Annotation-free quantification of RNA splicing using LeafCutter. *Nature genetics.* **50**, 151–158 https://doi.org/10.1038/s41588-017-0004-9 (2018).

18. Li, B. & Dewey, C. N. RSEM: accurate transcript quantification from RNA-Seq data with or without a reference genome. *BMC bioinformatics.* **12**, 323 https://doi.org/10.1186/1471-2105-12-323 (2011).
19. Bray, N. L., Pimentel, H., Melsted, P. & Pachter, L. Near-optimal probabilistic RNA-seq quantification. *Nature biotechnology.* **34**, 525–527 https://doi.org/10.1038/nbt.3519 (2016).
20. Patro, R., Duggal, G., Love, M. I., Irizarry, R. A. & Kingsford, C. Salmon provides fast and bias-aware quantification of transcript expression. *Nature methods.* **14**, 417–419 https://doi.org/10.1038/nmeth.4197 (2017).
21. Vitting-Seerup, K. & Sandelin, A. The Landscape of Isoform Switches in Human Cancers. *Mol Cancer Res.* **15**, 1206–1220 https://doi.org/10.1158/1541-7786.MCR-16-0459 (2017).
22. Zhang, C. *et al.* Computational identification and validation of alternative splicing in ZSF1 rat RNA-seq data, a preclinical model for type 2 diabetic nephropathy. *Scientific reports.* **8**, 7624 https://doi.org/10.1038/s41598-018-26035-x (2018).
23. Kahraman, A., Karakulak, T., Szklarczyk, D. & von Mering, C. Pathogenic impact of transcript isoform switching in 1,209 cancer samples covering 27 cancer types using an isoform-specific interaction network. *Scientific reports.* **10**, 14453 https://doi.org/10.1038/s41598-020-71221-5 (2020).
24. Schaub, A. & Glasmacher, E. Splicing in immune cells-mechanistic insights and emerging topics. *Int Immunol.* **29**, 173–181 https://doi.org/10.1093/intimm/dxx026 (2017).
25. Ip, J. Y. *et al.* Global analysis of alternative splicing during T-cell activation. *RNA.* **13**, 563–572 https://doi.org/10.1261/rna.457207 (2007).
26. Madeira, F. *et al.* The EMBL-EBI search and sequence analysis tools APIs in 2019. *Nucleic Acids Res.* **47**, W636–W641 https://doi.org/10.1093/nar/gkz268 (2019).
27. Mitchell, A. L. *et al.* InterPro in 2019: improving coverage, classification and access to protein sequence annotations. *Nucleic Acids Res.* **47**, D351–D360 https://doi.org/10.1093/nar/gky1100 (2019).
28. Guan, K. L. *et al.* Growth suppression by p18, a p16INK4/MTS1- and p14INK4B/MTS2-related CDK6 inhibitor, correlates with wild-type pRb function. *Genes Dev.* **8**, 2939–2952 https://doi.org/10.1101/gad.8.24.2939 (1994).
29. Okada, M. *et al.* The CENP-H-I complex is required for the efficient incorporation of newly synthesized CENP-A into centromeres. *Nat Cell Biol.* **8**, 446–457 https://doi.org/10.1038/ncb1396 (2006).
30. Foltz, D. R. *et al.* The human CENP-A centromeric nucleosome-associated complex. *Nat Cell Biol.* **8**, 458–469 https://doi.org/10.1038/ncb1397 (2006).
31. Eldridge, A. G. *et al.* The evi5 oncogene regulates cyclin accumulation by stabilizing the anaphase-promoting complex inhibitor emi1. *Cell.* **124**, 367–380 https://doi.org/10.1016/j.cell.2005.10.038 (2006).
32. Hsu, J. Y., Reimann, J. D., Sorensen, C. S., Lukas, J. & Jackson, P. K. E2F-dependent accumulation of hEmi1 regulates S phase entry by inhibiting APC(Cdh1). *Nat Cell Biol.* **4**, 358–366 https://doi.org/10.1038/ncb785 (2002).

33. Reimann, J. D. *et al.* Emi1 is a mitotic regulator that interacts with Cdc20 and inhibits the anaphase promoting complex. *Cell.* **105**, 645–655 https://doi.org/10.1016/s0092-8674(01)00361-0 (2001).
34. Lim, S. L. *et al.* HENMT1 and piRNA Stability Are Required for Adult Male Germ Cell Transposon Repression and to Define the Spermatogenic Program in the Mouse. *PLoS Genet.* **11**, e1005620 https://doi.org/10.1371/journal.pgen.1005620 (2015).
35. Azzam, R. *et al.* Phosphorylation by cyclin B-Cdk underlies release of mitotic exit activator Cdc14 from the nucleolus. *Science (New York, N.Y.).* **305**, 516–519 https://doi.org/10.1126/science.1099402 (2004).
36. Holt, L. J. *et al.* Global analysis of Cdk1 substrate phosphorylation sites provides insights into evolution. *Science (New York, N.Y.).* **325**, 1682–1686 https://doi.org/10.1126/science.1172867 (2009).
37. Shou, W. *et al.* Exit from mitosis is triggered by Tem1-dependent release of the protein phosphatase Cdc14 from nucleolar RENT complex. *Cell.* **97**, 233–244 https://doi.org/10.1016/s0092-8674(00)80733-3 (1999).
38. Ghezraoui, H. *et al.* 53BP1 cooperation with the REV7-shieldin complex underpins DNA structure-specific NHEJ. *Nature.* **560**, 122–127 https://doi.org/10.1038/s41586-018-0362-1 (2018).
39. Gupta, R. *et al.* DNA Repair Network Analysis Reveals Shieldin as a Key Regulator of NHEJ and PARP Inhibitor Sensitivity. *Cell* **173**, 972–988 e923, doi:10.1016/j.cell.2018.03.050 (2018).
40. Imai, K. *et al.* Human uracil-DNA glycosylase deficiency associated with profoundly impaired immunoglobulin class-switch recombination. *Nat Immunol.* **4**, 1023–1028 https://doi.org/10.1038/ni974 (2003).
41. Kavli, B. *et al.* hUNG2 is the major repair enzyme for removal of uracil from U:A matches, U:G mismatches, and U in single-stranded DNA, with hSMUG1 as a broad specificity backup. *J Biol Chem.* **277**, 39926–39936 https://doi.org/10.1074/jbc.M207107200 (2002).
42. Kovalev, G. I., Franklin, D. S., Coffield, V. M., Xiong, Y. & Su, L. An important role of CDK inhibitor p18(INK4c) in modulating antigen receptor-mediated T cell proliferation. *J Immunol.* **167**, 3285–3292 https://doi.org/10.4049/jimmunol.167.6.3285 (2001).
43. Hosokawa, H. *et al.* Gata3/Ruvbl2 complex regulates T helper 2 cell proliferation via repression of Cdkn2c expression. *Proceedings of the National Academy of Sciences of the United States of America.* **110**, 18626–18631 https://doi.org/10.1073/pnas.1311100110 (2013).
44. Gump, J., Turner, S. & Koh, J. The COOH terminus of p18INK4C distinguishes function from p16INK4A. *Cancer Res.* **61**, 3863–3868 (2001).
45. Jeffrey, P. D., Tong, L. & Pavletich, N. P. Structural basis of inhibition of CDK-cyclin complexes by INK4 inhibitors. *Genes Dev.* **14**, 3115–3125 https://doi.org/10.1101/gad.851100 (2000).
46. Li, J. *et al.* Tumor suppressor INK4: quantitative structure-function analyses of p18INK4C as an inhibitor of cyclin-dependent kinase 4. *Biochemistry.* **39**, 649–657 https://doi.org/10.1021/bi991281u (2000).

47. Liu, L. *et al.* Two Transcripts of FBXO5 Promote Migration and Osteogenic Differentiation of Human Periodontal Ligament Mesenchymal Stem Cells. *Biomed Res Int* 2018, 7849294, doi:10.1155/2018/7849294 (2018).
48. Snider, N. T. *et al.* Alternative splicing of human NT5E in cirrhosis and hepatocellular carcinoma produces a negative regulator of ecto-5'-nucleotidase (CD73). *Mol Biol Cell.* **25**, 4024–4033 https://doi.org/10.1091/mbc.E14-06-1167 (2014).
49. Panigrahi, S. *et al.* CD8(+) CD73(+) T cells in the tumor microenvironment of head and neck cancer patients are linked to diminished T cell infiltration and activation in tumor tissue. *Eur J Immunol.* https://doi.org/10.1002/eji.202048626 (2020).
50. Chan, A. M., Takai, S., Yamada, K. & Miki, T. Isolation of a novel oncogene, NET1, from neuroepithelioma cells by expression cDNA cloning. *Oncogene.* **12**, 1259–1266 (1996).
51. Schmidt, A. & Hall, A. The Rho exchange factor Net1 is regulated by nuclear sequestration. *J Biol Chem.* **277**, 14581–14588 https://doi.org/10.1074/jbc.M111108200 (2002).
52. Papadimitriou, E. *et al.* Differential regulation of the two RhoA-specific GEF isoforms Net1/Net1A by TGF-beta and miR-24: role in epithelial-to-mesenchymal transition. *Oncogene.* **31**, 2862–2875 https://doi.org/10.1038/onc.2011.457 (2012).
53. Zhang, C., Zhang, B., Lin, L. L. & Zhao, S. Evaluation and comparison of computational tools for RNA-seq isoform quantification. *BMC Genomics.* **18**, 583 https://doi.org/10.1186/s12864-017-4002-1 (2017).
54. Martinez, N. M. *et al.* Alternative splicing networks regulated by signaling in human T cells. *RNA.* **18**, 1029–1040 https://doi.org/10.1261/rna.032243.112 (2012).
55. Szabo, P. A. *et al.* Single-cell transcriptomics of human T cells reveals tissue and activation signatures in health and disease. *Nat Commun.* **10**, 4706 https://doi.org/10.1038/s41467-019-12464-3 (2019).
56. Kedzierska, K. *et al.* Quantification of repertoire diversity of influenza-specific epitopes with predominant public or private TCR usage. *J Immunol.* **177**, 6705–6712 https://doi.org/10.4049/jimmunol.177.10.6705 (2006).
57. Moon, J. J. *et al.* Naive CD4(+) T cell frequency varies for different epitopes and predicts repertoire diversity and response magnitude. *Immunity.* **27**, 203–213 https://doi.org/10.1016/j.immuni.2007.07.007 (2007).
58. Carr, H. S., Morris, C. A., Menon, S., Song, E. H. & Frost, J. A. Rac1 controls the subcellular localization of the Rho guanine nucleotide exchange factor Net1A to regulate focal adhesion formation and cell spreading. *Mol Cell Biol.* **33**, 622–634 https://doi.org/10.1128/MCB.00980-12 (2013).
59. Carr, H. S., Zuo, Y., Oh, W. & Frost, J. A. Regulation of focal adhesion kinase activation, breast cancer cell motility, and amoeboid invasion by the RhoA guanine nucleotide exchange factor Net1. *Mol Cell Biol.* **33**, 2773–2786 https://doi.org/10.1128/MCB.00175-13 (2013).
60. Menon, S., Oh, W., Carr, H. S. & Frost, J. A. Rho GTPase-independent regulation of mitotic progression by the RhoGEF Net1. *Mol Biol Cell.* **24**, 2655–2667 https://doi.org/10.1091/mbc.E13-01-0061 (2013).

61. Bono, M. R., Fernandez, D., Flores-Santibanez, F., Rosemblatt, M. & Sauma, D. CD73 and CD39 ectonucleotidases in T cell differentiation: Beyond immunosuppression. *FEBS Lett.* **589**, 3454–3460 https://doi.org/10.1016/j.febslet.2015.07.027 (2015).
62. Deaglio, S. *et al.* Adenosine generation catalyzed by CD39 and CD73 expressed on regulatory T cells mediates immune suppression. *J Exp Med.* **204**, 1257–1265 https://doi.org/10.1084/jem.20062512 (2007).
63. Csoka, B. *et al.* Adenosine A2A receptor activation inhibits T helper 1 and T helper 2 cell development and effector function. *FASEB J.* **22**, 3491–3499 https://doi.org/10.1096/fj.08-107458 (2008).
64. Wilson, J. M. *et al.* The A2B adenosine receptor impairs the maturation and immunogenicity of dendritic cells. *J Immunol.* **182**, 4616–4623 https://doi.org/10.4049/jimmunol.0801279 (2009).
65. Dustin, M. L., Tseng, S. Y., Varma, R. & Campi, G. T cell-dendritic cell immunological synapses. *Curr Opin Immunol.* **18**, 512–516 https://doi.org/10.1016/j.coi.2006.05.017 (2006).
66. Beavis, P. A., Stagg, J., Darcy, P. K. & Smyth, M. J. CD73: a potent suppressor of antitumor immune responses. *Trends Immunol.* **33**, 231–237 https://doi.org/10.1016/j.it.2012.02.009 (2012).
67. Jin, D. *et al.* CD73 on tumor cells impairs antitumor T-cell responses: a novel mechanism of tumor-induced immune suppression. *Cancer Res.* **70**, 2245–2255 https://doi.org/10.1158/0008-5472.CAN-09-3109 (2010).

Figures

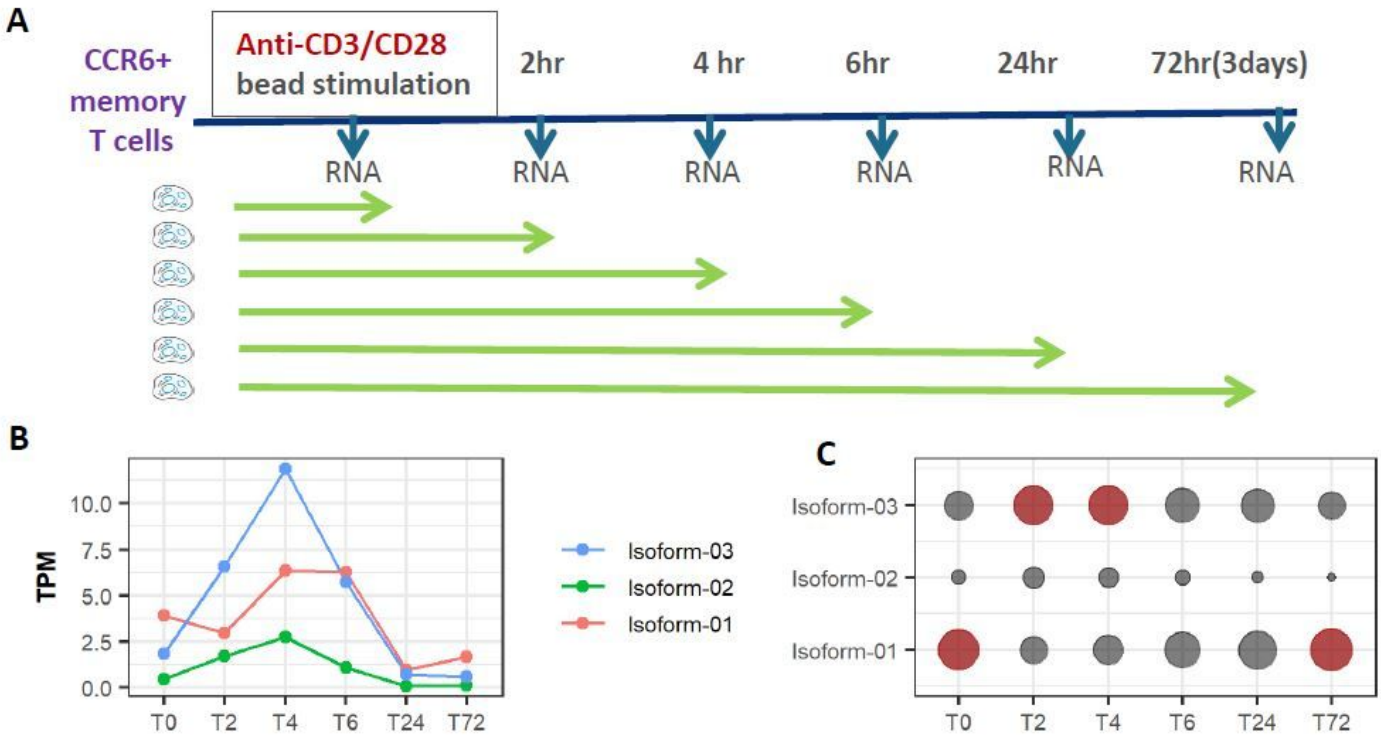

Figure 1

Experimental design and analysis protocol for isoform switch. (A) memory T cells were stimulated by anti-CD3/CD28 beads, and RNA samples were collected and sequenced at different time points; (B) the expression of different isoforms during T cell activation; and (C) the relative abundance of individual isoforms at each time point with dominant isoforms colored red.

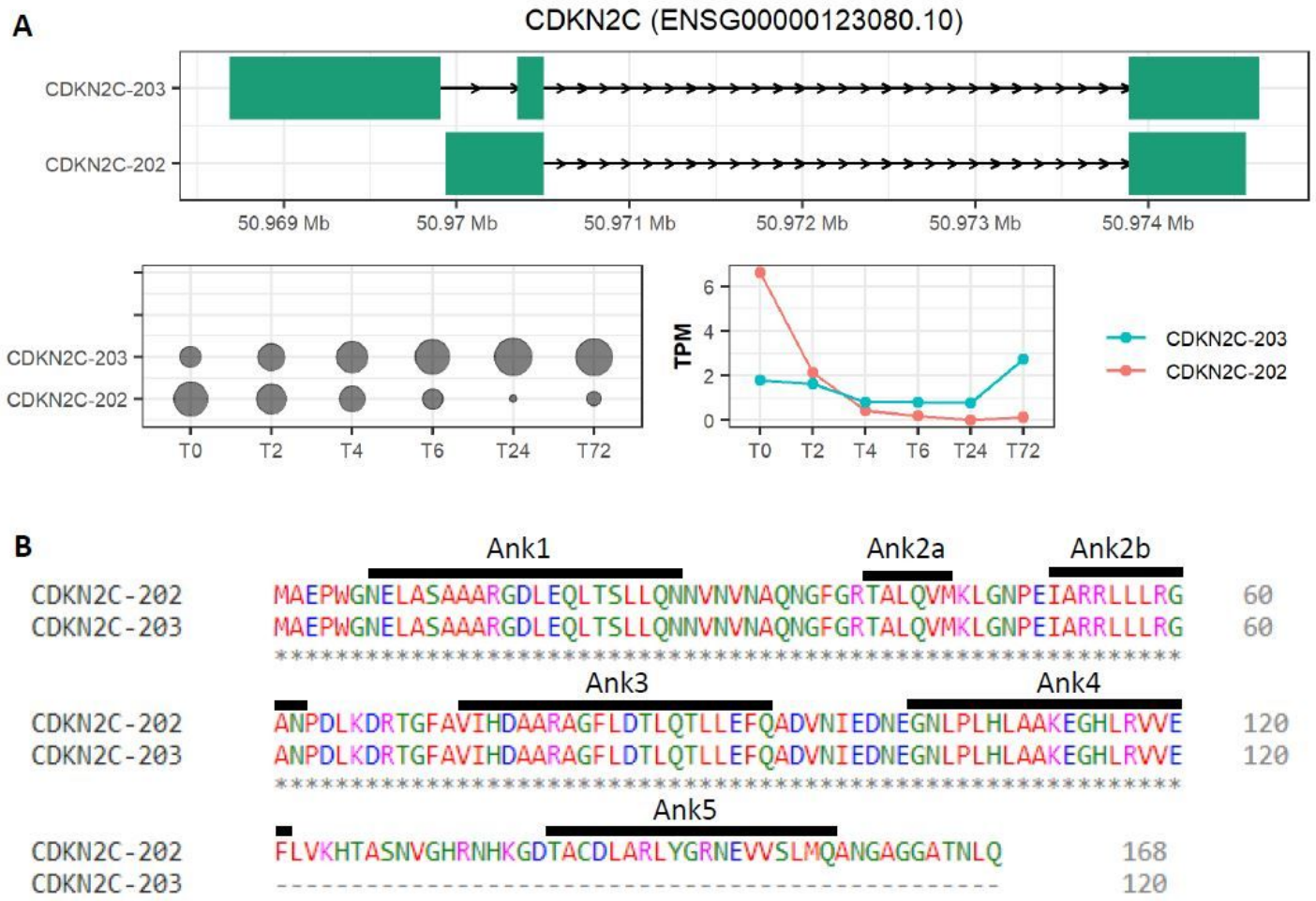

Figure 2

Isoform switch in CDKN2C (Cyclin-dependent kinase inhibitor 2C). (A) CDKN2C has two expressed protein coding isoforms, CDKN2C-202 and CDKN2C-203. The CDKN2C-202 is the dominant isoform at early time points, but CDKN2C-203 becomes the dominant one at 72hr; (B) ClustalW alignment of CDKN2C-202 and -203 isoforms with sequences encoding ankyrin repeats marked. CDKN2C-203 lacks Ank5 domain.

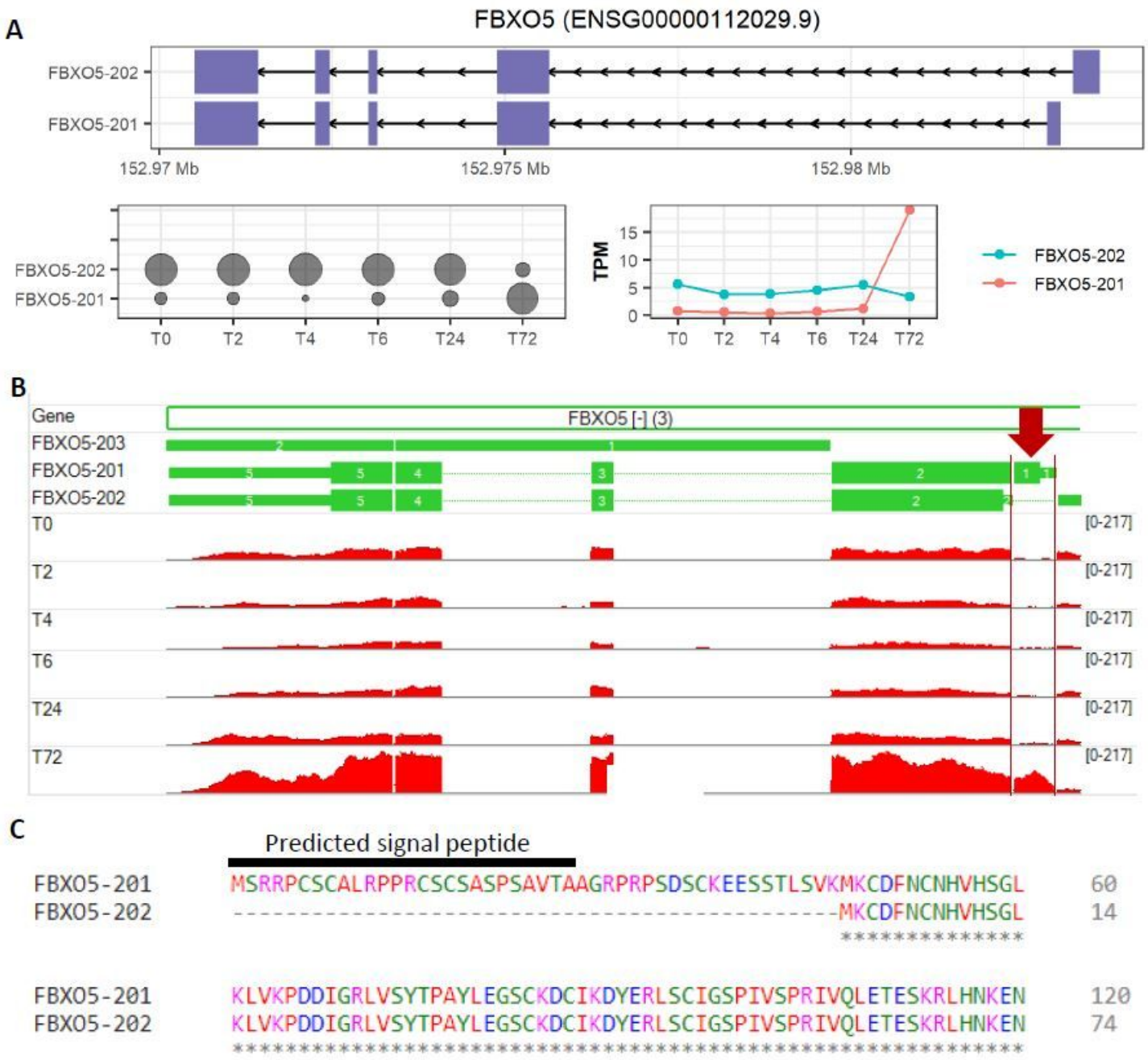

Figure 3

Isoform switch in FBXO5 (F-box protein 5). (A) FBXO5 has two expressed protein coding isoforms, FBX05-201 and FBX05-202. FBXO5 is encoded at the minus strand, and these two isoforms differ only at exon #1 and share the rest common exons. The FBX05-202 is the dominant isoform at early time points, but FBX05-201 becomes the dominant isoform at 72hr; (B) read coverage profiles support the high expression level of FBX05-201 at 72hr; (C) partial Clustal Omega alignment of FBXO5-201 and -202 splice variants with the predicted signal peptide encoded by amino acids 1-26 marked.

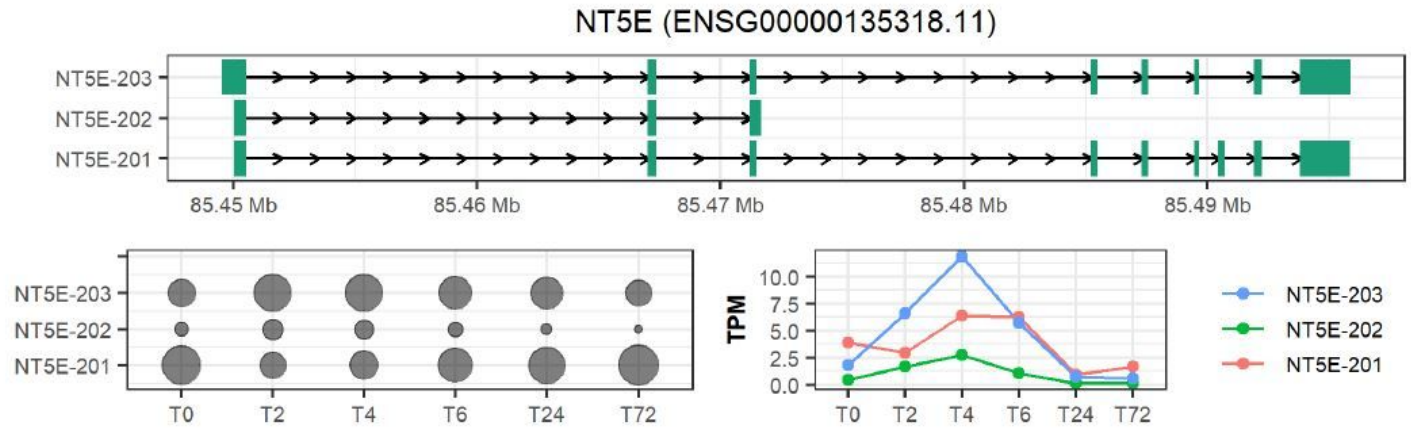

Figure 4

Isoform switch in NT5E (5'-nucleotidase ecto) or CD73 (cluster of differentiation 73). NT5E-201 encodes canonical CD73, denoted as CD73L, while the NT5E-203 transcript is predicted to encode a shorter protein CD73S, lacking amino acids 404–453, encoded by the missing exon 7. The dominant isoform is NT5E-203 at 2 and 4hr, but it is NT5E-201 at 0 and 72hr.

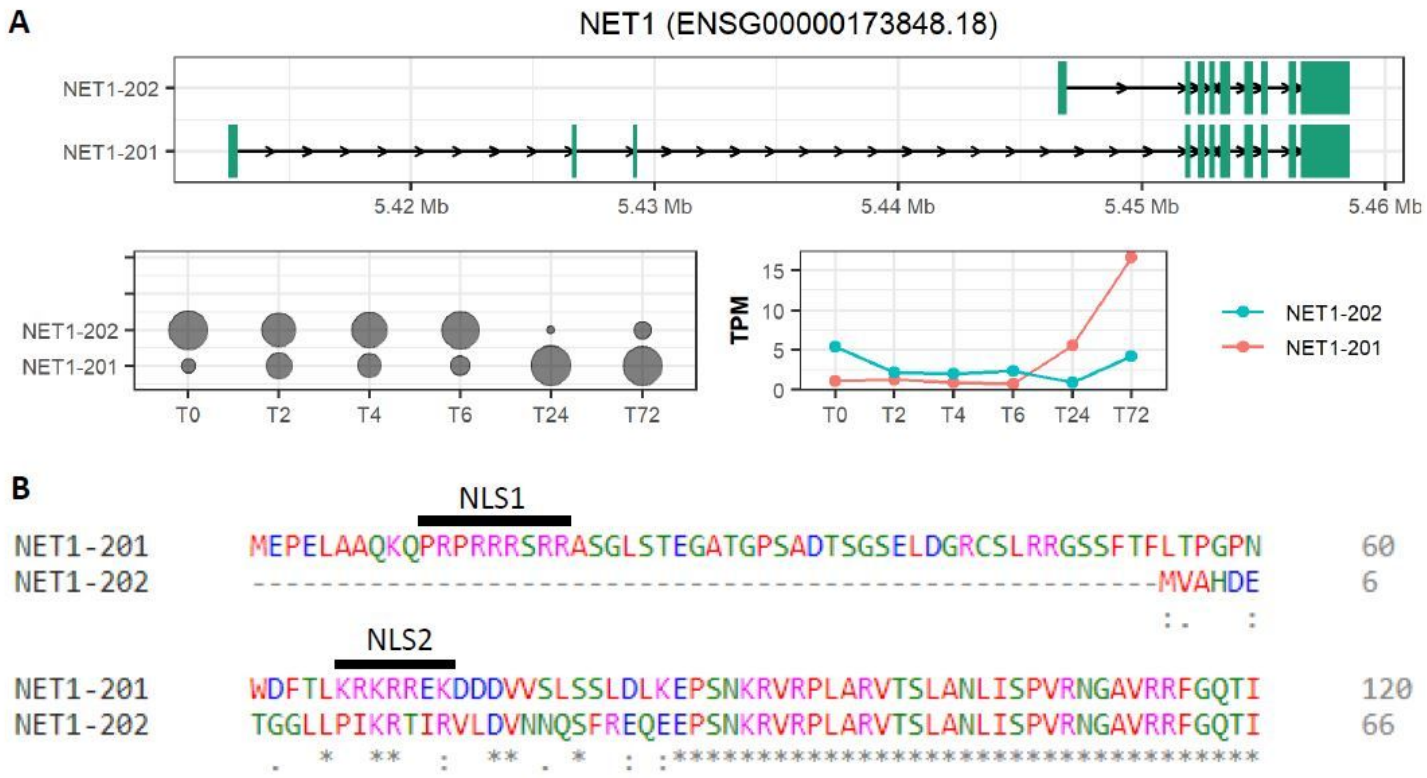

Figure 5

Isoform switch in NET1 (Neuroepithelial cell transforming 1). (A) Compared with NET1-202, the expression for NET1-201 is low at early time points but increases significantly to become the dominant isoform at 24 and 72hr. The two isoforms differ at the 5’ end with two more exons (exon #2 and #3) spliced into NET1-201. (B) The N-terminal portion of a Clustal Omega alignment of NET1-201 and -202 showing exclusion of the nuclear localization sequences (NLS) from the NET1-202 splice variant.

Supplementary Files

This is a list of supplementary files associated with this preprint. Click to download.

- Figs.supp.pdf